Surface electromagnetic waves in lossy media for environmental sensing applications

Igor I. Smolyaninov*[a], Vera N. Smolyaninova[b]
[a]Saltenna LLC, 1751 Pinnacle Drive, Suite 600 McLean, VA 22102-4903 USA; [b]Dept. of Physics Astronomy and Geosciences, Towson University, 8000 York Rd., Towson, MD 21252 USA

ABSTRACT

We demonstrate that gradual interfaces between lossy conductive media support propagation of a novel kind of surface electromagnetic wave, which is different from the more well-known surface plasmon polaritons. Potential applications of these novel surface waves to monitor water surface and the seawater-ice interface, as well as other environmental sensing applications in the RF and optical domain are discussed.

Keywords: surface electromagnetic wave, environmental sensing, nanophotonics, water, ice

1. INTRODUCTION

Surface plasmon polaritons (SPP) are widely used in environmental sensing in the visible frequency range [1]. They are surface electromagnetic wave (SEW) solutions of the macroscopic Maxwell equations which arise at sharp interfaces between good metals and dielectrics [2]. Very recently it was demonstrated that a different kind of SEW may exist at a gradual interface between two different lossy electromagnetic media [3]. If a gradual transition region ε(z) is assumed to exist (as illustrated in Fig. 1) at the boundary separating two media, the wave equation for the TM polarized SEW mode may be written as

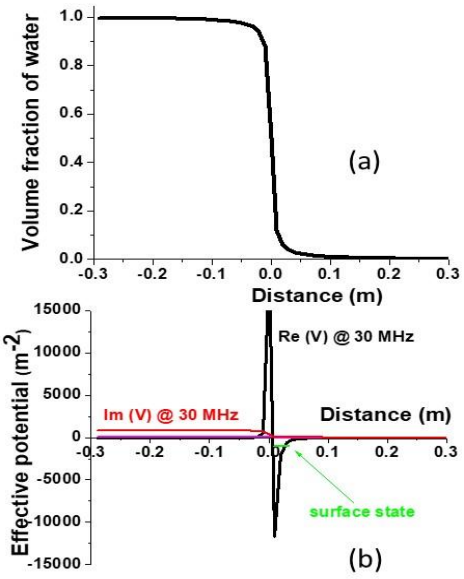

Figure 1. (a) Assumed model of the ~ 5 cm wavy transition layer near the air-water interface. (b) Real (black) and imaginary (magenta and red) parts of the effective potential energy near the air-water interface calculated for the 30 MHz frequency band using Eq.(1). The modeled water salinity was 0.2% (magenta) and 3.5% (red). The SEW state is indicated by the green arrow.

*igor.smolyaninov@narelab.com; www.saltenna.com

SPIE-CLP Conference on Advanced Photonics 2023, edited by Anatoly V. Zayats, Xiao-Cong Yuan, Proc. of SPIE Vol. 12746, 1274604 · © 2023 SPIE
0277-786X · doi: 10.1117/12.2688833

$$-\frac{\partial^2\psi}{\partial z^2}+\left(-\frac{\varepsilon(z)\omega^2}{c^2}-\frac{1}{2}\frac{\partial^2\varepsilon}{\varepsilon\partial z^2}+\frac{3}{4}\frac{\left(\partial\varepsilon/\partial z\right)^2}{\varepsilon^2}\right)\psi=-\frac{\partial^2\psi}{\partial z^2}+V(z)\psi=-k^2\psi \quad , \tag{1}$$

which coincides with a one-dimensional Schrödinger equation in which the wave function is introduced as $\psi=\varepsilon^{1/2}E_z$, and E_z is the electric field component of the surface wave, which is perpendicular to the interface. The effective potential energy V(z) in Eq.(1) depends on the gradient terms, and the effective total energy $-k^2$ is defined by the SEW wave vector k along the interface. As demonstrated in [3], the gradient terms may become dominant in Eq.(1), leading to appearance of unconventional propagating surface wave solutions even in the case of a gradual interface between two strongly lossy materials in which ε(z) is large and imaginary.

In particular, such novel SEW solutions were predicted and experimentally observed at interfaces between water and air [4], and water and sea floor [5]. It should be noted that such novel SEW solutions differ substantially from Zenneck waves, which are known to appear even in the sharp interface approximation [6]. The generic feature of Zenneck waves is their radiative character, which is due to their wave vector k being smaller than the wave vector of photons in the adjacent dielectric medium. Unlike Zenneck waves, the wave vector k of the novel SEW solutions is typically larger than the photon wave vector (see Fig. 1b), which makes them similar to SPPs in this respect.

2. SENSING APPLICATIONS OF SURFACE ELECTROMAGNETIC WAVES AT WATER-AIR AND WATER-ICE INTERFACES

The similarity between SPPs and the surface electromagnetic waves at various water interfaces make them a very good candidate for water and ice monitoring applications. Indeed, sensing applications of SEWs are based on strong exponential field enhancement at the interface, which in the case of SPPs leads to their sensitivity to even sub-monolayers of various surface adsorbates [1]. Therefore, a similar enhanced sensitivity to surface contaminations may be predicted for SEW-based water and ice sensors.

The theoretically predicted exponential enhancement of SEW field near the water-air interface was indeed observed in our experiments conducted in the RF domain, as illustrated in Figs. 2 and 3. As illustrated in Fig. 2, excitation and propagation of SEW RF signals has been extensively tested in the well-controlled swimming pool environment. The received SEW signal was studied as a function of depth and distance underwater. The typical received signal intensity as a function of z measured across the air-water interface is shown in Fig.3. The same antenna was used below and above

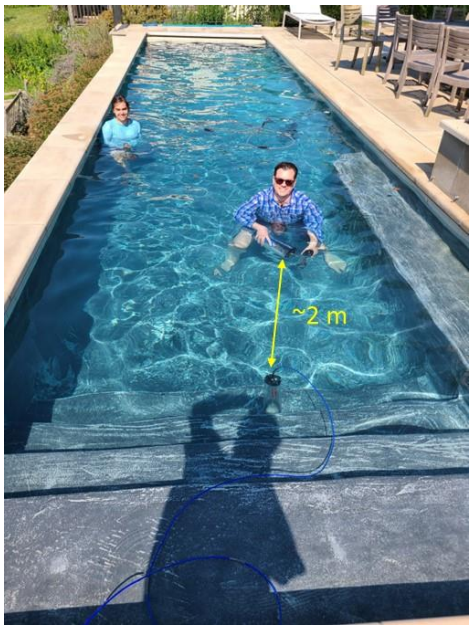

Figure 2. Picture of the pool test site. The 30 MHz SEW signal is transmitted using an underwater surface wave antenna using 20 mW (13dBm) transmit power. The measured water salinity in the pool was 0.2%, which corresponds to 20 cm skin depth at 30 MHz.

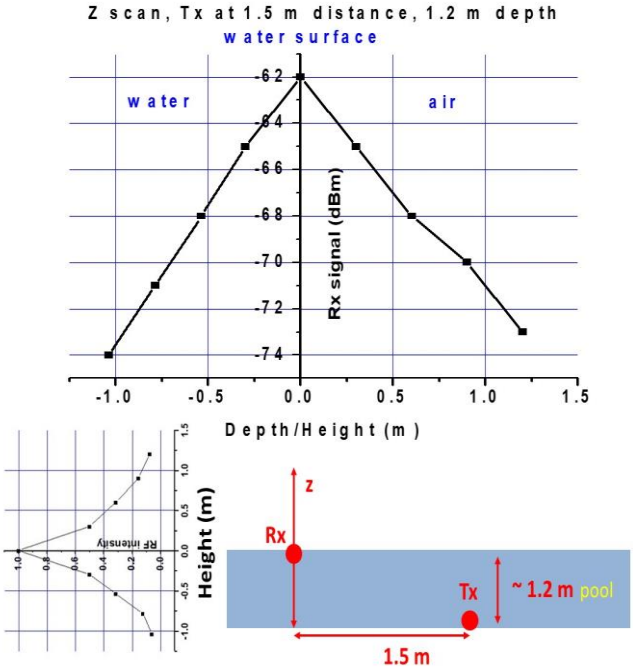

Figure 3. The top plot shows typical SEW signal dependence as a function of z measured across the air-water interface in the experimental geometry shown schematically in the bottom figure. The plot in the inset on the left shows the same measured SEW signal in linear scale. The measured field profile matches the anticipated theoretical profile of the SEW signal.

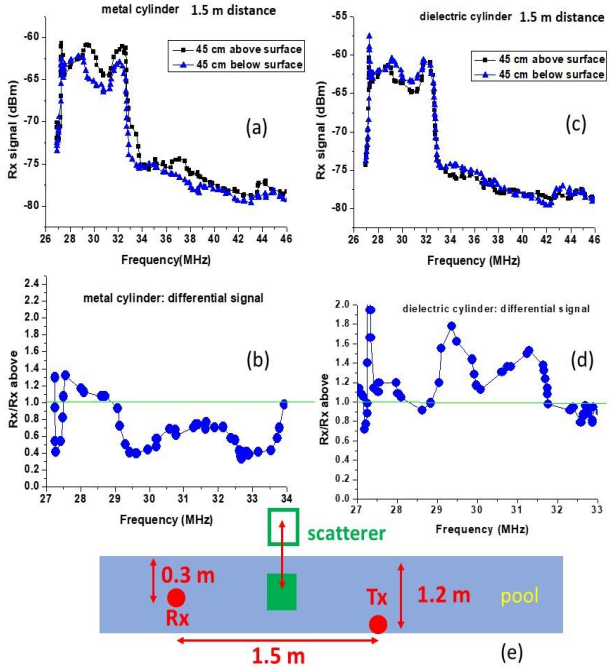

Figure 4. (a) SEW signal measured with and without 0.3 m diameter metal cylinder underwater. (b) Ratio of the SEW signals with and without the metal cylinder. (c) Rx signal measured with and without 0.3 m diameter dielectric cylinder underwater. (d) Ratio of the SEW signals with and without the dielectric cylinder. (e) Schematic diagram of the experimental geometry.

the interface. As expected, the measured field profile matched the theoretical SEW field distribution, which falls off exponentially away from the water-air interface into both media [3]. Note that this experiment also proves that the SEW transmission system is quite efficient at communicating through the water-air interface, which is known to be extremely difficult for acoustical and optical wireless communication systems.

Using the same experimental system, we were also able to study SEW scattering by underwater objects. The scattering effect appears to be rather strong near surface and, unlike the acoustic detection systems, the SEW scattering strongly depends on the dielectric properties of an underwater object. As illustrated in Fig.4, placing a metal cylinder underwater in the path of SEW propagation led to attenuation of the received signal. On the other hand, placing a similar shape dielectric cylinder underwater led to the increase of SEW signal. The opposite SEW scattering effects depending on the dielectric properties of an object located underwater is clearly seen from the comparison of Figs 4b and 4d.

The obtained experimental results are consistent with our theoretical study of SEW scattering by underwater objects, which is presented in Fig. 5. To illustrate the practicality of SEW imaging, even in such conditions as imaging under ice, we have performed the numerical simulations at considerably lower SEW frequency of 10 KHz, so that underwater detection at tens of meters scale would be feasible. The schematic geometry of our study performed using COMSOL Multiphysics electromagnetic solver is shown in Fig. 5a together with the map of total SEW field distribution. It roughly corresponds to the geometry of our experiments shown in Fig. 4e with an addition of surface ice layer. These theoretical results indeed demonstrate a very similar dielectric contrast in SEW scattering. While metal objects obstruct SEW penetration, dielectric objects placed underwater facilitate SEW signal propagation, which leads to increased SEW signal.

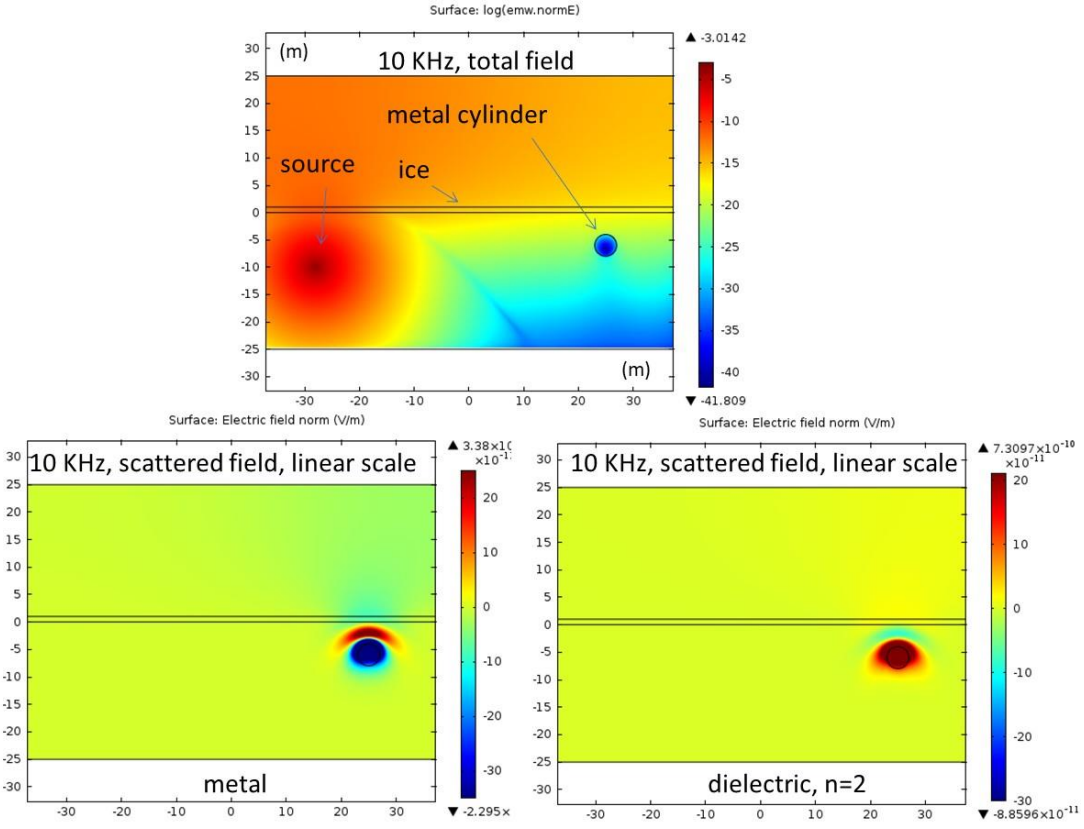

Figure 5. Numerical simulations of SEW scattering by underwater under-ice objects using COMSOL Multiphysics. (a) Model geometry representing an ice-covered sea surface shown together with the total SEW field distribution. The spatial scales are given in meters. (b) Scattering SEW signal in the vicinity of a metal cylinder. A perfect metal was assumed in these simulations. (c) Scattering signal in the vicinity of a dielectric cylinder having the dielectric permittivity ε=4. The SEW frequency in both cases is 10 KHz.

Our theoretical results on SEW scattering by under-ice objects indicate that this novel technique may potentially be used to study Antarctic ice melting, which remains a great global challenge for the humanity [7]. The SEW field at the seawater-ice interface must be extremely sensitive to the ice surface roughness, which typically indicates the onset of ice melting.

3. NOVEL SURFACE ELECTROMAGNETIC WAVE GEOMETRIES FOR VISIBLE AND UV LIGHT APPLICATIONS

We should also understand based on Eq.(1) that similar SEW modes must also exist at gradual interfaces between either two dielectrics or two metals, which may or may not be highly lossy. Indeed, in such cases the shape of the effective potential from Fig. 1b, which is mostly affected by the gradient terms, will look essentially similar. The only necessary condition for such modes to exist is that the loss tangent should not change considerably across the interface [8]. Therefore, TM polarized SEW solutions must also exist in the highly lossy dielectric cases in the UV range, which is quite typical for almost all known optical materials. Such SEW solutions will have a k vector larger than the k vector of photons in each neighboring medium, thus making them very similar to SPPs. The existence of such large k vector SEW modes in a large variety of dielectric samples may lead to interesting new possibilities in UV nanophotonics and environmental sensing. Unlike the typical plasmonic metals, which are not well suited for nanofabrication using the CMOS techniques, numerous silicon-based SEW geometries become possible. Indeed, around 300 nm wavelength of UV light, doping of silicon with various metals, such as nickel or titanium, changes the absolute magnitude of the dielectric constant of silicon, while it remains almost pure imaginary [9].

We have obtained strong evidence in favor of existence of such novel SEW modes in the UV-VIS domain on the example of silicon-titanium interface – see Fig.6. In this experiment we have studied UV transmission of an overlap region between a 260 nm thick silicon and a 230 nm thick titanium film. A stripe of enhanced transmission which goes in parallel with the silicon-titanium interface is clearly visible in Fig.6. According to the Fermi's golden rule, the increased

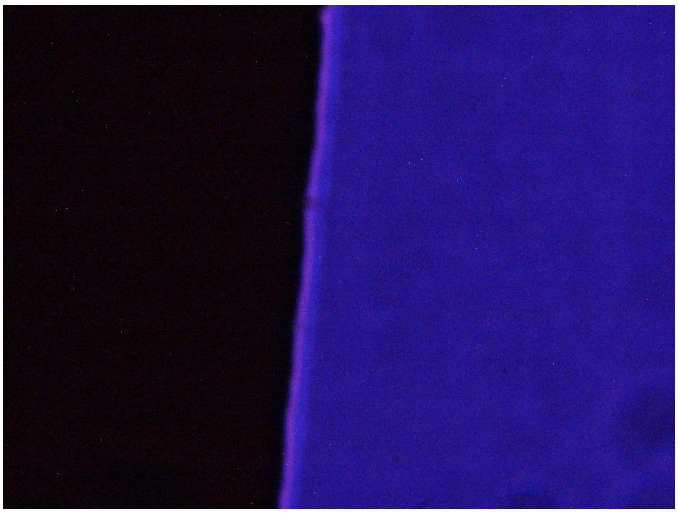

Figure 6. Transmission optical microscope image of an overlap region between a 260 nm thick silicon and a 230 nm thick titanium film. Note the stripe of enhanced transmission which goes in parallel with the silicon-titanium interface.

transmission of light at the silicon-titanium junction indicates an increased density of photonic states (DOS) in the general area of the junction, which become available to the photons tunneling through this thick composite conductive film. Therefore, a strong increase in light transmission near the Si/Ti junction is a rather strong indication in favor of the SEW interfacial modes.

4. CONCLUSIONS

In conclusion, we have demonstrated that gradual interfaces between lossy conductive media support propagation of novel surface electromagnetic waves in the RF, visible and UV domains. These novel SEW solutions are different from

the more well-known surface plasmon polaritons. On the other hand, because these novel surface waves share many important similarities with the conventional surface plasmons, such as strong exponential field enhancement at the interface, potential applications of the novel surface waves to monitor water surface and the seawater-ice interface, as well as other environmental sensing applications in the RF and UV-VIS domains look very promising.

REFERENCES

[1] Masson, J.-F., "Portable and field-deployed surface plasmon resonance and plasmonic sensors," Analyst 145, 3776-3800 (2020).

[2] Zayats, A. V., Smolyaninov, I. I., Maradudin, A., "Nano-optics of surface plasmon-polaritons", Physics Reports 408, 131-314 (2005).

[3] Smolyaninov, I. I., "Surface electromagnetic waves in lossy conductive media: tutorial", JOSA B 39, 1894-1901 (2022).

[4] Smolyaninov, I. I., Balzano, Q., Davis, C. C., Young, D., "Surface wave-based underwater radio communication", IEEE Antennas and Wireless Propagation Letters 17, 2503-2507 (2018).

[5] Smolyaninov, I. I., Balzano, Q., Kozyrev, A. B., "Surface electromagnetic waves at seawater-air and seawater-seafloor interfaces", IEEE Open Journal of Antennas and Propagation 4, 51-59 (2023).

[6] Michalski, K. A., Mosig, J. R., "The Sommerfeld half-space problem revisited: From radio frequencies and Zenneck waves to visible light and Fano modes," J. Electromagn. Waves Appl. 30, 1–42, (2016).

[7] Silvano, A., Rintoul, S. R., Peña-Molino, B., Hobbs, W. R., van Wijk, E., Aoki S., Tamura, T., Williams, G. D., "Freshening by glacial meltwater enhances melting of ice shelves and reduces formation of Antarctic Bottom Water", Science Advances 4, eaap9467 (2018).

[8] Smolyaninov, I. I., "Gradient-index nanophotonics", Journal of Optics 23, 095002 (2021).

[9] Amiotti, M., Borghesi, A., Guizzetti, G., Nava, F., "Optical properties of polycrystalline nickel silicides", Phys. Rev. B 42, 8939 (1990).